URSI GASS 2021, Rome, Italy, 28 August - 4 September 2021

Radio Frequency Engineering Advancements for the Ghana Radio Telescope

Mariet Venter*(1) and Jocias A. Malan(1)
(1) South African Radio Astronomy Observatory (SARAO), Cape Town, South Africa

Abstract

This paper presents recent radio frequency (RF) engineering work performed for the Ghana Radio Telescope, specifically concerning receiver and electromagnetic component design and analysis. An upgraded so-called Mark II receiver, currently nearing the end of its development phase, improves the bandwidth by approximately 100% and 30% for the 5 and 6.7 GHz bands, respectively. A proposed new wideband orthomode transducer (OMT) design is presented to replace the existing Intermediate Circular Orbit (ICO) satellite system components, which are known to add extra noise. Also contributing to the system noise temperature is the antenna and spillover temperatures. Electromagnetic simulation data is used to determine these parameters, showing that the antenna can contribute up to 32 K to the system noise temperature near the horizon. The resulting predicted sensitivity of the telescope is presented and is in the range of 4.6 to 5 m^2/K assuming a receiver temperature of 90 K and an aperture efficiency of 70%.

1 Introduction

The African Very Long Baseline Interferometry (VLBI) Network (AVN) is a Square Kilometre Array (SKA) programme, funded by the African Renaissance Fund (ARF) and led by the South African Radio Astronomy Observatory (SARAO). This programme aims to bring new science opportunities to participating countries and enable participation in SKA pathfinder development by among others, converting several large antennas into radio astronomy telescopes. A 32-m telecommunications dish in Kutunse, Ghana, has already been converted for operations at 5 and 6.7 GHz covering VLBI and the 6.7 GHz methanol line, respectively. Currently, various mechanical and radio frequency (RF) engineering upgrades are in development to further improve the telescope. This paper gives an overview of specific improved RF components as well as electromagnetic simulation analysis, which contributes to the overall understanding of the RF performance of the antenna.

2 Antenna Optics Overview

A detailed description of the Ghana Radio Telescope antenna optics is presented in [1] and only a short overview will be presented here for the reader's convenience. The Ghana Radio Telescope is shown in Fig. 1 and consists of a Cassegrain shaped dual-reflector system with four mirrors in a beam-waveguide (BWG). The 32 m primary reflector has an f/d of 0.32 and the Cassegrain focus is 0.84 m above the primary reflector vertex. The sub-reflector diameter is 2.90 m. Two flat and two concave mirrors are inside the BWG, reflecting the signal to the feed horn phase centre approximately 20 m below the primary reflector vertex.

Figure 1. The Ghana Radio Telescope at Kutunse.

3 Receiver

3.1 Limitations of Current Design

The feed horn is followed by three stages of the receiver in the signal chain. Currently, the first stage primarily comprises of the original Intermediate Circular Orbit (ICO) satellite system waveguide components, low noise amplifiers (LNAs) as well as noise diode modules. A physical representation of the ICO components is shown in Fig. 2. The polariser converts circularly polarised to linearly polarised signals. The orthomode transducer (OMT) separates the linearly polarised signals into horizontal and vertical polarisations which maps to left and right circular polarisation (LCP and RCP, respectively). This is done for both the 5 GHz and 6.7 GHz frequency bands independently, resulting in four outputs from the OMT. Waveguide bandpass filters (BPFs) interfaces with the OMT which reject out-of-band signals in both frequency bands. A dual cross-guided waveguide coupler allows for the injection of noise diode calibration signals as well as user-defined test signals before the input of the low noise amplifiers (LNAs).

Down-conversion to an intermediate frequency (IF) is performed using a two stage heterodyne architecture. The RF signal is down-converted to a first IF frequency of 2.9 GHz before being down-converted to the final IF of 600 MHz. A further complication of the current system is that the backend of the telescope comprises a Digital Base Band Converter (DBBC) VLBI backend recorder [2] which samples the IF at a rate of 1024 Msps and a ROACH1 (Reconfigurable Open Architecture Computing Hardware) [3] based backend which samples the IF at 800 Msps. This difference in IF frequencies result in a complicated switching architecture for the third stage of the receiver. The key specifications of the current receiver is summarised in Table 1.

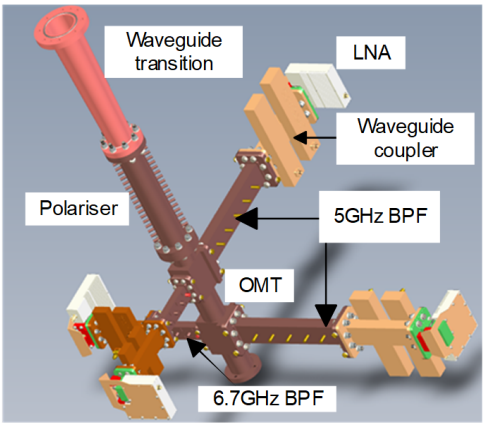

Figure 2. Graphical representation of the first stage of the current receiver with original ICO components.

Table 1. Current receiver specifications.

Specification	Value
5 GHz frequency range	4950 - 5014 MHz
6.7 GHz frequency range	6550 - 6850 MHz
DBBC IF	768 MHz
DBBC bandwidth	192 MHz
ROACH1 IF	600 MHz
ROACH1 bandwidth	300 MHz
T_{sys}	$\leq$ 100 K

The current receiver has several shortcomings including high internal and external complexity. There is a lack of firmware and software to support control and monitoring in order to facilitate self-diagnostics and reporting. This greatly limits remote support and on-site fault-finding and repair, which given the remoteness of the site, introduces more engineering effort and cost. The ICO components remained part of the current receiver as a compromise of convenience and to save time and cost. The station also originally hosted a transmitter that operated between the 5 and 6.7 GHz bands, prohibiting a wideband receiver that covered both bands simultaneously. However, it has been measured that the ICO OMT and polariser combination contributes loss to an order of 0.5 dB, which adds 35 K to the system noise temperature.

3.2 New Design and Proposed Wideband OMT

Given the limitations as outlined in the previous section, a new receiver will be implemented. The shortcomings will be met by among others, incorporating a controller into each stage to handle its own control and monitoring, changing the receiver architecture to single down-conversion architecture and incorporating an adjustable attenuator into the noise diode module. The ROACH1 based backend has been upgraded to a wideband ROACH2 [3] based backend which samples the IF at the same rate as that of the DBBC (1024 Msps). This change simplified the receiver architecture such that a common IF can be produced by the receiver instead of two different IF frequencies. The upgrade of the backend also allows for the RF bandwidths to be increased to the limit of the ICO frontend. The new bandwidth for the 5 GHz channel is 128 MHz (currently 64 MHz) and 400 MHz for the 6.7 GHz channel (currently 300 MHz). The key specifications of the new receiver is summarised in Table 2.

Table 2. New receiver specifications.

Specification	Value
5 GHz frequency range	4917 - 5045 MHz
6.7 GHz frequency range	6550 - 6950 MHz
IF output	768 MHz
IF bandwidth	400 MHz
T_{sys}	$\leq$ 100 K

A new OMT is also proposed to eventually replace the ICO components over the wider frequency band of 4.6 GHz to 6.9 GHz (40% bandwidth). This is possible since the transmitter mentioned in the previous section is no longer operational. The OMT will interface directly with the feed horn and deliver two linear polarisations. A return loss of at least 15 dB across the band is required, with cross-polarisation isolation of more than 30 dB between the output ports.

A design to satisfy these requirements is shown in Fig. 3. Four rectangular probes soldered to coaxial connectors, are arranged orthogonally in a circular waveguide of 54.1 mm diameter. The probes have a length and width of 9.6 mm and 3.7 mm, respectively. This OMT design is very compact compared to the ICO assembly and has good simulated characteristics over the 4.5 to 7.0 GHz band. The return loss is limited to approximately 20 dB across the 4.6 to 6.9 GHz band and the cross-polarisation level below -54 dB. Of course, wideband 180° couplers will also have to be designed to combine the output ports, which will add some unwanted loss, which then increases the system noise temperature. A proposed coupler based on the design in [4] with optimisation performed in CST [5] for the purposes described in this paper, is shown in Fig. 3. A double sided single layer Rogers 6010 (ε_r = 10.7) substrate of 0.635 mm thickness is used. The size of the substrate in length and width is 23.47 and 20.74 mm, respectively.

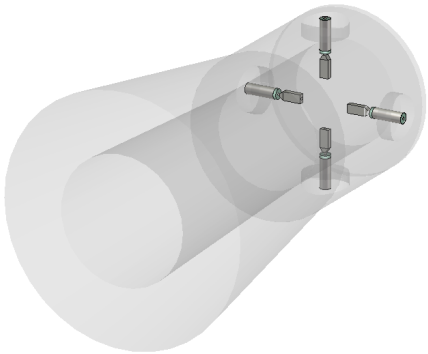

Figure 3. Proposed new OMT design to replace the ICO components.

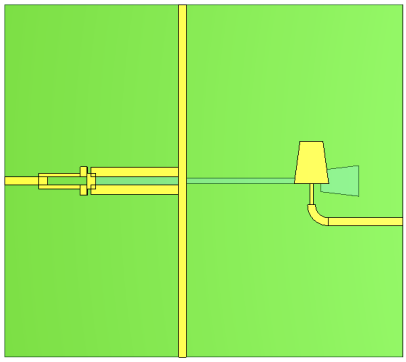

Figure 4. Proposed 180° coupler design. Top layer is shown in gold.

The OMT and coupler designs are integrated in CST to calculate the resulting return and insertion loss, as shown in Fig. 5. Port 1 and 2 are the single output ports of the couplers whereas Port 3 and 4 are the two polarisations at the input of the OMT waveguide. Here the couplers are excited to produce a return and insertion loss over the entire band of better than 15 and 0.2 dB, respectively.

4 Antenna Noise Temperature

Another contributing factor to the system noise temperature is the antenna noise temperature. The sensitivity of a radio telescope is determined by the system noise temperature (the sum of the receiver temperature and the antenna noise temperature) and the aperture efficiency. It is shown in [6] that the ideal (not including surface errors etc.) aperture efficiency of the Ghana Radio Telescope is approximately 90% due to the highly shaped primary and sub-reflectors. However, in order to estimate the sensitivity of the antenna, the system noise temperature also needs to be calculated. The antenna noise temperature includes noise contribution from atmospheric, ground and cosmic sources as described in [7].

The antenna noise temperature is calculated in the form of a tipping curve using GRASP [8] simulation data at 5 and 6.7 GHz, over an elevation of 0 to 80 degrees (where 90 degrees

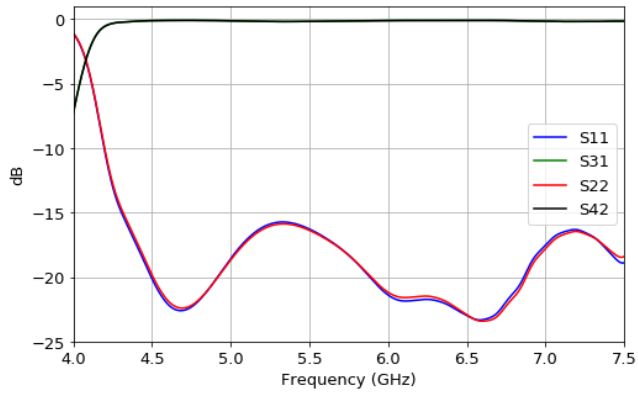

Figure 5. The simulated s-parameters for the OMT and couplers integrated design.

is the horizon). Methods described in [9] are used to perform the calculations. The spillover temperature is obtained by subtracting the brightness models from the antenna temperature. The curves are shown in Fig. 6 and the resulting sensitivity in Fig. 7. An aperture efficiency of 70% is assumed, as determined by microwave holography and a receiver temperature of 90 K, as typically measured for the current receiver. It is expected that T_{spill} will be slightly lower for lower elevation angles as more spillover is seeing the cooler sky temperature. The struts and BWG are not included in the calculations.

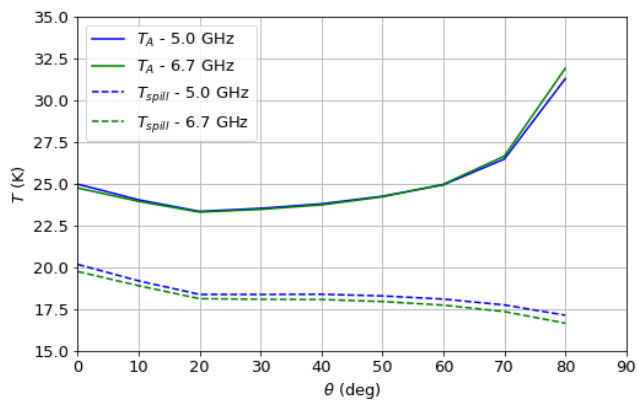

Figure 6. The simulated antenna noise temperature T_{A} and spillover temperature T_{spill} for the Ghana Radio Telescope.

5 Conclusion

This paper presents recent RF design and analysis performed for the Ghana Radio Telescope, which includes a new receiver and proposed wideband OMT. Future work includes the verification of the new receiver as well as physically installing and testing on site. The OMT and wideband coupler will be manufactured as a prototype to replace the ICO components with the longterm possibility of cryogenic cooling.

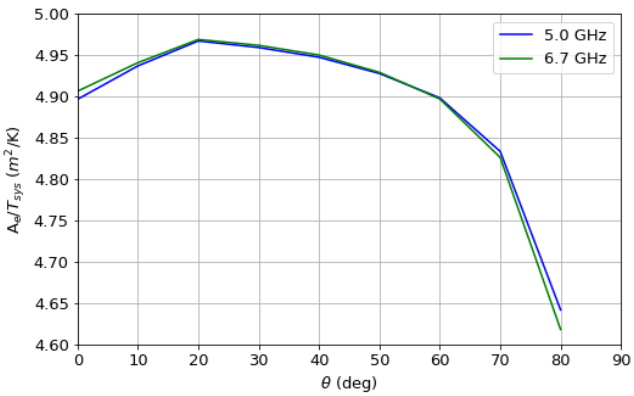

Figure 7. The simulated Ghana Radio Telescope sensitivity over elevation assuming a receiver temperature of 90 K and an aperture efficiency of 70%.

6 Acknowledgements

The authors would like to acknowledge Professor Dirk de Villiers from Stellenbosch University for his contribution to the antenna noise temperature and spillover temperature calculations. The authors also acknowledges support by the South African Department of International Relations and Cooperation (DIRCO), the Department of Science and Innovation (DSI) and the National Research Foundation (NRF).

References

[1] M. Venter and P. Bolli, ”Electromagnetic modelling of the 32-m Ghana radio telescope,” *2017 IEEE Radio and Antenna Days of the Indian Ocean (RADIO)*, Cape Town, 2017, doi: 10.23919/RADIO.2017.8242212.

[2] Digital Base Band Converter (DBBC) used for VLBI, [Online] Available: www.hat-lab.cloud/dbbc2.

[3] Collaboration for Astronomy Signal Processing and Electronics Research (CASPER), [Online] Available: casper.ssl.berkeley.edu/wiki/Hardware.

[4] M. A. Ashraf, Z. O. Al-Hekail, M. A. Alkanhal and A. Sebak, "Design of a slot-coupled Ultra-Wideband 180° hybrid coupler," *2012 15 International Symposium on Antenna Technology and Applied Electromagnetics*, Toulouse, 2012, pp. 1-4, doi: 10.1109/ANTEM.2012.6262319.

[5] Dassault Systemes, CST Studio Suite Version 2020.07, dated 10 July 2020.

[6] M. Venter and P. Bolli, “Electromagnetic analysis and preliminary commissioning results of the shaped dual-reflector 32-m Ghana radio telescope,” *IOP Conference Series: Materials Science and Engineering*, **321**, March 2018, doi: 10.1088/1757-899x/321/1/012003.

[7] G. C. Medellin, “Antenna noise temperature calculations,” *SKA Memo 95*, pp. 1–13, July 2007.

[8] GRASP, TICRA, Copenhagen, Denmark, [online] Available: www.ticra.com.

[9] D. I. L. de Villiers and R. Lehmensiek, "Rapid Calculation of Antenna Noise Temperature in Offset Gregorian Reflector Systems,” *IEEE Transactions on Antennas and Propagation*, **63**, 4, pp. 1564-1571, April 2015, doi: 10.1109/TAP.2015.2399933.